RSC Advances

REVIEW

View Article Online
View Journal | View Issue

Cite this: *RSC Adv.*, 2024, **14**, 446

A comprehensive review of synthesis kinetics and formation mechanism of geopolymers

Ahmer Ali Siyal, *[a] Radin Maya Saphira Radin Mohamed, *[a] Rashid Shamsuddin [b] and Mohd Baharudin Ridzuan*[a]

Geopolymers are synthesized by alkali or acid activation of aluminosilicate materials. This paper critically reviews the synthesis kinetics and formation mechanism of geopolymers. A variety of mechanistic tools such as Environmental Scanning Electron Microscopy (ESEM) and *in situ* Energy Dispersive X-ray diffractometry (EDXRD), *in situ* Isothermal Conduction Calorimetry (ICC), *in situ* Attenuated Total Reflectance Fourier Transform Infrared Spectroscopy (ATR-FTIR), ^{1}H low-field Nuclear Magnetic Resonance (NMR) and Isothermal Conduction Calorimetry (ISC), and others and phenomenological models such as the John–Mehl–Avrami–Kolmogorov (JMAK) model, modified Jandar model, and exponential and Knudson linear dispersion models were used to study the geopolymerization kinetics and many mechanisms were proposed for the synthesis of geopolymers. The mechanistic tools and phenomenological models provided new insights about geopolymerization kinetics and formation mechanisms but each of the techniques used possesses some limitations. These limitations need to be removed and new methods or techniques must be developed to overcome these challenges and get more detailed information about all types of geopolymers. The formation mechanism consists of three to four stages such as dissolution of raw materials, polymerization of silica and alumina, condensation, and reorganization. The Si/Al ratio above the Si/Al ratio of reactants is more suitable and it increases the rate or degree of reaction and produces a higher compressive strength geopolymer. The Na/Al ratio of 1,

Received 12th September 2023
Accepted 20th November 2023

DOI: 10.1039/d3ra06205h

rsc.li/rsc-advances

[a]*Micropollutant Research Centre (MPRC), Institute for Integrated Engineering (I2E), Universiti Tun Hussein Onn Malaysia (UTHM), 86400 Parit Raja, Batu Pahat, Johor, Malaysia. E-mail: ahmer@uthm.edu.my; maya@uthm.edu.my; mdbahar@uthm.edu.my*

[b]*HICoE, Centre for Biofuel and Biochemical Research (CBBR), Institute for Sustainable Living, Department of Chemical Engineering, Universiti Teknologi PETRONAS, 32610 Bandar Seri Iskandar, Perak Darul Ridzuan, Malaysia*

Ahmer Ali Siyal

Dr Ahmer Ali Siyal is a chemical engineer by profession. He possesses teaching, research, and industrial experiences. He got his PhD in Chemical Engineering from Universiti Teknologi Petronas, Malaysia. With more than eight years of teaching and research experience, he is now trying to solve the problems of micropollutant removal from diverse industrial effluents. He is currently working as a Postdoctoral Fellow at the Micropollutants Research Centre (MPRC), Faculty of Civil Engineering and Built Environment, Universiti Tun Hussein Onn Malaysia. He has published 29 Scopus-indexed papers in reputed peer-reviewed journals during his research career.

Radin Maya Saphira Mohamed Radin

Radin Maya Saphira Radin Mohamed is an Associate Professor and currently held as Head of the Micropollutant Research Centre (MPRC) at the Institute for Integrated Engineering (I2E), Universiti Tun Hussein Onn Malaysia. She graduated her PhD in Environmental Engineering (Greywater Recycling/Reuse for Irrigation) at Murdoch University, Perth, Australia, in 2011. MEng (Research) in Civil Engineering (Environment) in 2004 and BSc (Hons) in Industrial Chemistry from Universiti Technology of Malaysia in 2001. Her current research looks at the environmental issues related to water quality, greywater and decentralized wastewater management and resource recovery, and the exploration of innovative technology for safe disposal.

water-to-solid (W/S) ratio of 0.30–0.45, a temperature in the range of 30 °C to 85 °C, and a curing time of 24 hours are the best for the synthesis of geopolymers. The growing demand for geopolymers in various fields requires the development of new advanced techniques for further understanding of kinetics and mechanisms for tailoring the properties of geopolymers for specific applications.

1. Introduction

The increase in industrialization is posing threats to the environment in terms of the by-products and waste generated by industry. One way to decrease the quantity of these by-products or waste is to select those processes that generate minimum by-products or waste. The other way is to produce useful materials using those by-products and waste; this can eliminate the environmental hazards associated with their disposal. The awareness about the quantity of solid waste generated and its hazardous effects on human health has built a demand to find new ways of utilizing this waste to produce valuable economy-generating products possessing good properties as well as diverse applications.[1] Technology that can utilize this waste and produce valuable product materials that can be used for various applications is highly required. A technology known as geopolymerization has emerged to handle these issues and produce valuable materials that possess properties superior to conventional materials and can be used in several applications. Geopolymers are low-cost and environmentally friendly green materials, which are produced from the source materials containing appreciable amounts of silica and alumina.

Glukhovsky[2] in the 1950s in the former Soviet Union (USSR) developed alkali-activated cement using slag containing a large amount of calcium. Davidovits in 1979 in France started similar work and synthesized alkali-activated cements using a calcium-free system of calcined clay and named them geopolymers. Geopolymers are synthesized through alkali or acid activation of aluminosilicate source materials. Metakaolin, fly ash, and ground granulated blast furnace slag (GGBFS) are commonly used for the synthesis of geopolymers. Sodium hydroxide (NaOH), potassium hydroxide (KOH), and phosphoric acid as activating solutions and sodium silicate (Na_2SiO_3) and potassium silicate ($K_2Si_2O_5$) as silica sources are used for the synthesis of geopolymers. The structure of the reaction product or gel of these materials is similar to organic thermoset polymers, so they are also termed inorganic polymers.[3] Geopolymerization involves dissolution, gelation, and condensation reactions occurring concurrently to produce the geopolymer.[4] Alkali dissolves the aluminosilicate to form free AlO_4 and SiO_4 tetrahedral units. During the reaction, water releases and the SiO_4 and AlO_4 tetrahedral units link in an alternative fashion and produce polymorphic precursors (–SiO_4–AlO_4–,SiO_4–AlO_4–SiO_4–, or –SiO_4–AlO_4–SiO_4–SiO_4–) through sharing of all oxygen atoms between two tetrahedral units and forming an amorphous to semi-crystalline geopolymer in which alkali metal cations charge balances the tetrahedral Al sites.[5] The properties of geopolymers are dependent on the raw materials, compositions, and curing conditions.[6,7] Geopolymers possess the properties of rapid setting and attaining high final strength,[8] superior thermal and chemical resistance,[9–11] low permeability,[12] and heavy metal wastes stabilization or immobilization.[13] Geopolymers are used in various fields such as construction,[14,15] wastewater treatment,[16,17] immobilization of hazardous compounds,[18,19] coatings,[20,21] preparation of slow-release fertilizers,[7,22–24] catalysis,[25,26] and carbon dioxide (CO_2) capture.[27,28]

The understanding of synthesis kinetics is very important for designing of new materials and the optimization of existing materials as it controls the microstructure and properties of the

Rashid Shamsuddin

Before teaching, Dr Rashid Shamsuddin worked in various engineering industries in the Middle East, Malaysia, and New Zealand. He graduated with a PhD degree in Materials and Processing from the University of Waikato, New Zealand. As an academic, he is currently actively involved in lecturing and R & D in the Chemical Engineering Department, Universiti Teknologi Petronas, Malaysia. His teaching subjects include Thermodynamics, Materials Science & Engineering, Environmental Chemical Engineering, HSE, and Workplace Safety in Malaysia. His active consultancy and research projects include biogas and biofertilizers from waste sources and synthesizing various adsorbents for wastewater treatment.

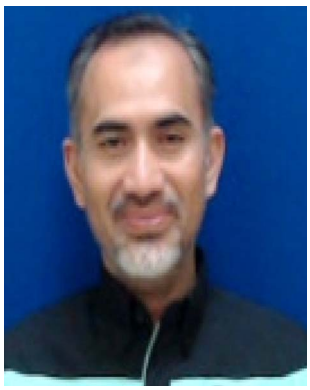

Mohd Baharudin Bin Ridzuan

Mohd Baharudin Bin Ridzuan had his PhD in Civil Engineering in 2022, Universiti Tun Hussein Onn Malaysia. M.Eng. in Civil Engineering, 2005, Kolej Universiti Tun Hussein Onn Malaysia and B.Eng (Hons). in Civil Engineering & Structure, 1999, Universiti Kebangsaan Malaysia. Currently, he is a senior lecturer at the University Tun Hussein Onn Malaysia. He is involved in the environmental engineering field of research, mainly on composite adsorbents for wastewater and leachate treatment.

product materials.[29] In the first two decades of the 21st century, research on geopolymer early age kinetics started to develop an understanding of the chemical reactions occurring during geopolymerization and the mechanisms involved in the formation of geopolymers. Few review papers on geopolymers such as mechanisms of geopolymerization and the factors affecting its development,[13] the structure and properties of clay based cements,[30] methods to evaluate and quantify the geopolymerization reactivity of waste-derived aluminosilicate precursor in alkali-activated material: a state of the art review,[31] phosphate-based geopolymers: a critical review[32] and on the advances in the synthesis and applications of geopolymers have been published.[33] However, no review has focused on the synthesis kinetics and formation mechanism of geopolymers.

This paper critically reviews the synthesis kinetics and formation mechanism of geopolymers. More than one hundred and fifty studies on geopolymers have been included in this review and around thirty studies conducted on geopolymerization kinetics and formation mechanism have been critically analyzed. It includes the introduction of the raw materials used, the critical review of the kinetics and mechanism, and the factors affecting the kinetics and mechanism of geopolymers. The future perspectives and challenges in the geopolymerization kinetics and formation mechanisms are also discussed.

2. Raw materials

The silica and alumina rich materials possessing pozzolanic properties are used to produce geopolymers. Metakaolin, fly ash, GGBFS, and RHA are commonly used for the synthesis of geopolymers. The use of fly ash, GGBFS, and RHA for the synthesis of geopolymer reduces the cost as they are by-product materials. The synthesis of geopolymers is shown in Fig. 1.

Fly ash is a by-product of thermal power plants. It is considered as a most complex anthropogenic source of pozzolans due to the presence of a variety of components. Pozzolans are the silica or silica and alumina materials which only show cementitious properties when activated in a finely divided form with alkali hydroxide at room temperature and moisture conditions.[34] The term mainly refers to the reaction of pozzolanic materials in finely divided form with calcium hydroxide ($Ca(OH_2)$) in the presence of water to produce materials possessing cementitious properties. The mineral composition of the inorganic part of coal determines the chemical composition of fly ash. Fly ash contains oxidized compounds of silicon (Si), aluminum (Al), iron (Fe), and calcium (Ca) around 90% while other elements such as sodium (Na), magnesium (Mg), titanium (Ti), potassium (K), and sulphur (S) are in small amounts.[35] Fly ash is composed of an organic part (char), an inorganic part (amorphous and crystalline mineral matter), and a fluid part (liquid, gas, and gas–liquid inclusions).[36] American Society of Testing Materials (ASTM) classifies fly ash into two classes such as F and C depending on the cumulative contents of silica, alumina, and ferrous oxide. The sum of silica, alumina, and ferrous oxide is above 70% for class F fly ash and in the range of 50–70% for class C fly ash.[37] Both classes of fly ash are commonly used for geopolymer synthesis.

Metakaolin is a dehydroxylated pozzolanic material which is produced by thermal activation of kaolin clay.[4] Kaolin consists of 40–70% of kaolinite (hydrated aluminum disilicate-$Al_2SiO_5(OH)_4$) and other minerals include muscovite-like micas and rutile and the quartz.[38] It is one of the most widely used mineral for various applications and its world output exceeds 25 million tones.[39] The heating of kaolin above 550 °C breaks its structure in which silica and alumina layers crumple and they lose their long-range order. The resulting material is highly reactive transition amorphous phase with pozzolanic and hydraulic reactivity which is suitable for cementing applications.[40,41] The calcination causes reorganization in the Al–O network while the Si–O network remains the same. The temperature from 650 °C to 900 °C is used in calcination of

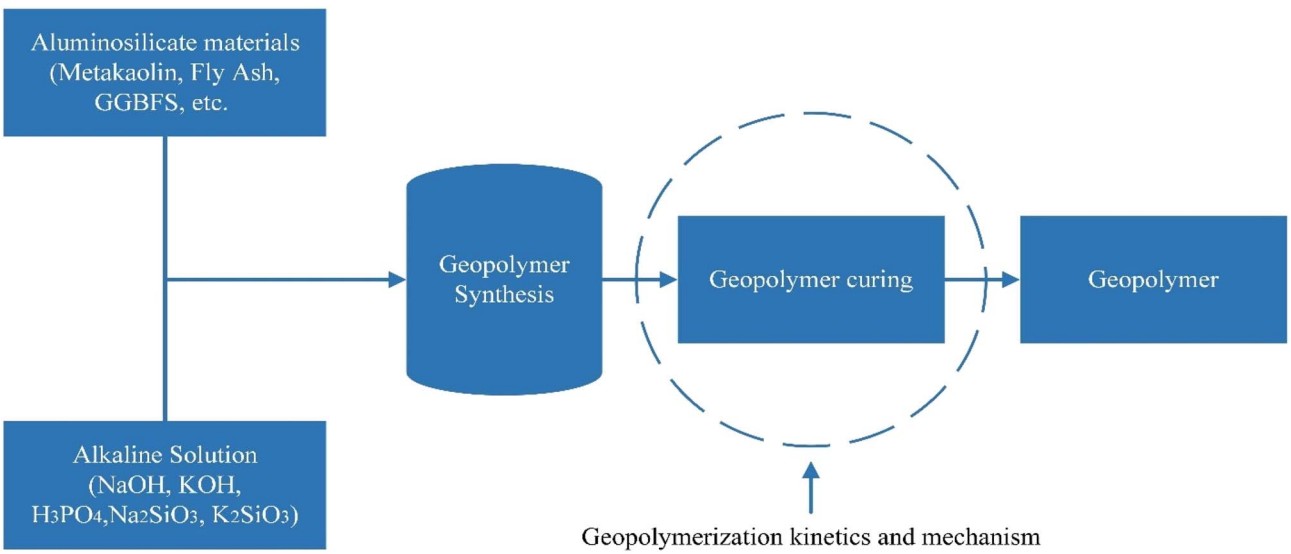

Fig. 1 Synthesis of geopolymers using aluminosilicate and alkaline solution.

Table 1 Chemical composition of aluminosilicate source materials

	Chemical composition				
Source material	SiO_2 (%)	Al_2O_3 (%)	Fe_2O_3 (%)	Others	Ref.
Fly ash	60–65	25–30	6–15	CaO, MgO, K_2O, TiO_2, SO_3	35
Metakaolin	50–55	40–45	—	Fe_2O_3, TiO_2, CaO, MgO	46
GGBFS	28–38	8–24	—	CaO and MgO	49
RHA	90–95	—	—	Carbon, CaO and K_2O	56
Mine tailings	64.81	7.08	4.33	CaO, MgO, SO_3, Na_2O, K_2O	60
Red mud (RM)	12.83	20.26	33.39	Na_2O, P_2O_5, CaO, SO_3, TiO_2, MgO	61
Coal gangue (CG)	45.69	22.21	5.44	Na_2O, P_2O_5, CaO, SO_3, TiO_2, MgO	61
Natural pozzolan feldspar	55.73	13.27	3.80	CaO, MgO, SO_3, Na_2O, K_2O	62
Calcinated alunite (CA)	44.32	39.6	0.63	CaO, MgO, Na_2O, K_2O, TiO_2, SO_3	63
Volcanic ash (Z_G)	41.36	15.41	12.88	MnO, TiO_2, MgO, CaO, Na_2O, P_2O_5, Cr_2O_3, K_2O	64
Iron ore tailings (IOT)	34.72	16.22	12.31	MgO, CaO, Na_2O, K_2O, MnO, TiO_2	65

kaolin. Metakaolin can also be produced by heating of indigenous lateritic soils (600–750 °C) and heating of waste sludge from paper recycling industry.[42–44] The nature and richness of clay minerals in the raw material, calcination conditions, and product fineness influence the pozzolanic properties of metakaolin. Metakaolin contains SiO_2 in the range of 50–55% and Al_2O_3 in the range of 40–45% and small amounts of other compounds such as Fe_2O_3, TiO_2, CaO, and MgO.[45] Metakaolin requires higher amount of water due to its fine particle size.[46]

Granulated blast furnace slag is produced during water quenching of slag in the steel industry as a by-product. The grinding of gypsum with slag makes it Ground Granulated Blast Furnace Slag (GGBFS). It can be used as a substitute material to improve the strength, permeability, and corrosion resistance of materials.[47,48] It contains SiO_2, Al_2O_3, CaO, and MgO as the major components.[49] The reactivity of GGBFS depends on its phase composition and glass structure. Calcium rich GGBFS can be used for the increase of compressive strength and setting time of fly ash geopolymers through the formation of aluminum modified calcium silicate hydrate (C-A-S-H) along with geopolymer gel (N-A-S-H) and compaction of microstructure.[50–52] GGBFS is suitable for the synthesis of geopolymers and specifically for high temperature applications.[53] According to ASTM C989, the reactivity of GGBFS is expressed in terms of slag activity index (SAI) which has been defined for Portland cement.[54] The other forms of slag such as ferrochrome slag (FS), ladle furnace slag (LFS), and furnace metallurgical slag (FMS) are also used for synthesis of geopolymers.

Rice husk (RH) is a protective cover of rice grains obtained during milling of the rice. The ash produced after burning of RH in the boiler is called Rice husk ash (RHA).[55] It has been noticed that after burning the rice husk, 20% of the rice husk retains in the final stage as rice husk ash. RHA contains 90–95 wt% silica (amorphous and partly crystalline), the amorphous to crystalline ratio depends on the temperature and burning time.[56] Carbon is the main impurity while it also contains K and Ca. RHA contains very light weight and porous particles which results in low unit weight and high external surface area.[57] The silica in amorphous form in RHA can be utilized as a pozzolanic material. RHA contains 20% ash content which is higher than other biomass fuels and it is affected by the type of rice, geographical location, and climate condition.[58,59] The presence of a high amount of amorphous silica makes it suitable for several applications. The low particle size (<50 μm), irregular shape, and porosity makes it suitable for use as a filler in polymers. It can also be used as a filler in cement and fertilizer, catalyst carrier and in the production of pure silica, silica gels, geopolymers, and filled polymers.[66,67] RHA can be used in the synthesis of geopolymers for increasing the silica content and it can also be used as a main raw material with the addition of external alumina for the synthesis of geopolymers. RHA has been used in the fly ash based geopolymer for enhancing the Si/Al ratio.[68] Table 1 shows the chemical composition aluminosilicate source materials, some other alumina and silica rich materials such as palm oil fuel ash, red mud, activated bentonite clay, clays, volcanic ash, bagasse bottom ash, loess powder, and gold mining wastes *etc.* are also used for the synthesis of geopolymers.

The silica and alumina are the main compounds required for the synthesis of geopolymers which are present in aluminosilicate materials. All aluminosilicate materials containing appreciable contents of silica and alumina can be used for the synthesis of geopolymers but if the content of silica or alumina is low then it can be increased by the addition of external silica or alumina. Metakaolin, fly ash, GGBFS, and RHA are generally used for the synthesis of geopolymers while various other aluminosilicate source materials have been introduced for the synthesis of geopolymers.

3. Geopolymerization kinetics

Kinetics is used to understand the reactions occurring and the mechanisms involved in the conversion of reactants into products. Monitoring of the changes taking place during geopolymerization and the mechanism involved in the transformation of raw materials into hardened products are very important for tailoring the properties of the final product. The kinetics approaches can be divided into two types: mechanistic and phenomenological. The kinetics studied using mechanistic

tools or equipment is known as mechanistic kinetics and the kinetics determined using models is called phenomenological kinetics. The phenomenological models are very helpful in the case of complex systems involving different phases and multi-step processes.

3.1 Mechanistic kinetics

Many mechanistic studies have been conducted to determine the kinetics of geopolymers. The formation of amorphous gels was observed during initial 4 hours of curing of geopolymers using Environmental Scanning Electron Microscopy (ESEM) and *in situ* Energy Dispersive X-Ray Diffractometry (EDXRD).[69,70] The rate of reaction decreased with the increase of silica content of a metakaolin based geopolymer.[71] In ESEM, after 30 minutes of reaction, sponge-like amorphous gel begin to appear which precipitated on metakaolin particles and small amount of gel filled the spaces between metakaolin particles. After 1.5 hours more gel produced in the voids available and extended outside. The amorphous gel was produced and covered the free space available after 4 hours of reaction, and the microstructure became more compact. K/Al and Si/Al ratios of the final products in case of K-PS geopolymers were 0.99 and 1.49 which are close to theoretical values for geopolymer. The XRD analysis showed only sponge-like amorphous gel while some peaks in XRD spectra were observed due to kaolin and quartz which were already present in metakaolin in crystalline form. It was noticed that Na based geopolymer reacted rapidly as compared to K based geopolymer that was due to actual capability of cations; Na^+ increases solubility and K^+ enhances condensation. The mixed sodium and potassium-activated geopolymer with moderate SiO_2/Al_2O_3 ratio showed similar behavior to pure Na or K geopolymer of higher SiO_2/Al_2O_3 ratio. The step in the Na-geopolymer lasted longer than K-geopolymer and this step was the change of mechanism from dissolution, orientation, and precipitation to transformation of newly produced gel to a more ordered and stable form. The activation energy of geopolymerization reaction was $E_a = 31.5$ kJ mol^{-1}. The combination of ESEM and EDXRD tools provided valuable in-depth information about the geopolymerization kinetics but the main drawback of both ESEM and EDXRD techniques is that they can only detect changes occurring during early stages of geopolymer formation.

Two peaks in geopolymer activated using lower temperature (20–30 °C) while three peaks in geopolymer activated using higher alkali concentration (10–12 M) and higher temperature (35–40 °C) were detected using *in situ* Isothermal Conduction Calorimetry (ICC) as shown in Fig. 2. Peak I was due to dissolution of metakaolin to produce Si and Al. Peak II was related to polymerization of Si and Al to produce aluminosilicate oligomers (O) which instantly polymerize to produce geopolymeric fragments (P) and protozeolitic nuclei (N) which will further produce polymer gels (G) and crystallized phases (Z). Peak III was due to reorganization and crystallization of produced geopolymers.[72,73] Only two peaks were detected in case of sodium silicate activated metakaolin geopolymers and no any crystalline products were observed after 3 days of curing.[74] Sodium showed more influence on geopolymerization as compared to temperature and soluble silica for NaOH activated metakaolin based geopolymers. The time needed to reach the maximum rate of heat evolution for peak I is 5 minutes for all systems studied irrespective of the temperature, while it varies for Peak II with the reaction temperature. The increase of reaction temperature shortened the time required to reach the maximum rate of heat evolution for Peak II. This technique provided good information about kinetics of metakaolin geopolymers, but it has some limitations for geopolymers prepared using fly ash and slag. The main limitation is that the thermochemical parameters of reactants and products required for data quantification are not available for slag and fly ash geopolymers and the estimation is difficult because these materials contain variety of components, and their nature is very complex, so this technique is not viable for fly ash and slag based geopolymer systems.

The X-ray pair distribution function analysis was conducted to determine the nano-structural changes occurring during geopolymerization. The data obtained was converted from 2D to 1D and then pair distribution function (PDF) was determined. The obtained PDF data was converted to nearest neighbor T–O (T stands for tetrahedral Si or Al), O–O, and T–T correlations. The geopolymer obtained through silicate activation of metakaolin remained amorphous during geopolymerization while the structure of hydroxide activated slag sample began to crystallize at some point during curing. The extent of reaction was faster for silicate activated metakaolin as compared to hydroxide activated metakaolin while for slag-based samples hydroxide activated sample was faster than silicate activated sample. The silica caused nucleation in the gel far from the dissolving particles surface in case of slag based geopolymer systems. It was observed that the presence of free silica in activating solution resulted in the higher dissolution of metakaolin during early reaction period but decreased the extent of reaction because of the dense morphology of the geopolymer paste.[75] The alkali and alkali silicate activated metakaolin and slag based geopolymers showed different behaviors. The extent of reaction was fast for silicate-activated metakaolin geopolymer as compared to hydroxide activated metakaolin geopolymer while it was fast for hydroxide activated slag geopolymer as compared to silicate activated slag geopolymer.

Another study conducted using the same technique to determine the effect of calcium on metakaolin/slag based geopolymer systems used atom–atom correlations occurring during geopolymer synthesis up to 128 days.[76] It was observed that in silicate activated metakaolin, as the reaction preceded the correlation due to Al–O decreased for 10.1 hours which indicated rapid dissolution of metakaolin but for 2–3 days the rate of structural changes slowed due to constrained nature of aluminosilicate gel. This behavior was because when metakaolin dissolved, the new phase of geopolymer material produced on partially dissolved metakaolin caused a decrease in the further dissolution of metakaolin. Initially gel 1 was formed which then transformed to a more ordered gel 2, so in case of silicate activated metakaolin, the aluminosilicate gel precipitated on partially dissolved metakaolin, and it took more

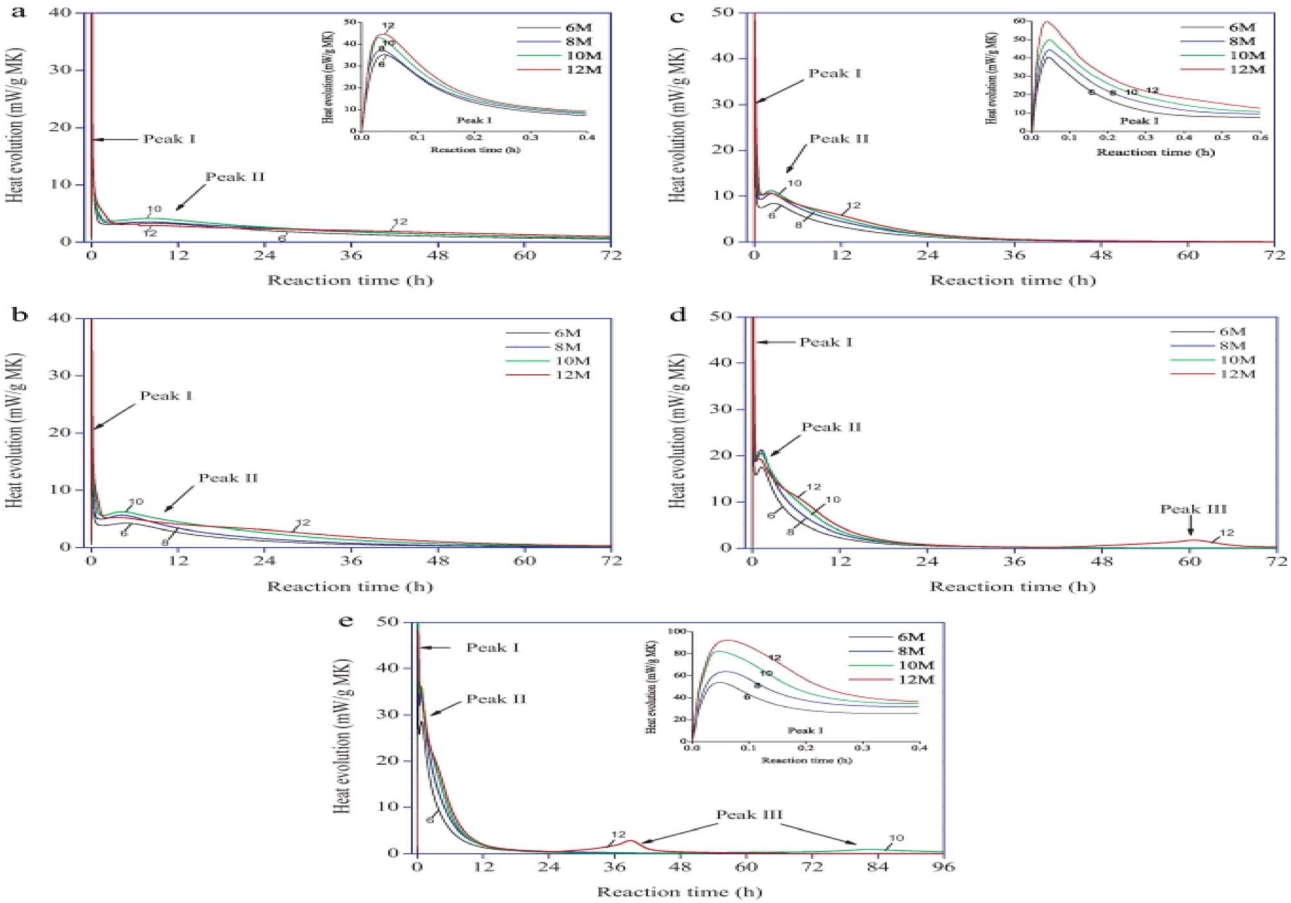

Fig. 2 Effects of NaOH concentration on the heat evolution of metakaolin geopolymers at (a) 20 °C, (b) 25 °C, (c) 30 °C, (d) 35 °C, and (e) 40 °C.[72]

time to transform into a more ordered gel 2. It was observed that more Ca–O correlations were occurring in the hydroxide activated systems as compared to silicate activated systems in metakaolin and slag based geopolymers. Silica increased the rate of reaction of metakaolin based geopolymers during an initial 10.1 hours. No changes in the peaks were observed during the initial 3 hours of reaction which was due to the induction period. This induction behavior was also observed in other studies.[6,77] This study provided a good understanding of the geopolymerization kinetics on nanoscale level. The limitation of this technique is that when crystals start to appear in case of hydroxide activated slag geopolymers, further data quantification becomes very difficult.

A kinetics study conducted using *in situ* Attenuated Total Reflectance Fourier Transform Infrared Spectroscopy (ATR-FTIR) showed the formation of Al-rich gel through the shifting of main (Si–O–T, T-tetrahedral Al, or Si) band to lower wavenumber for 36–48 hours as shown in Fig. 3(A and B). The *in situ* data obtained from the ATR-FTIR spectra was used in the functional group analysis to monitor the changes occurring in the main band during geopolymerization. After 72 hours of reaction, the main peak shifted to 958 cm^{-1} and this peak was also observed at the same position after 200 days which showed that no changes were occurred after 3 days of geopolymerization reaction.[78] The induction or delay period was detected during geopolymerization of hydroxide activated geopolymer sample. Two peaks can be seen in Fig. 3(B) at a time of 0 hours which were due to silicate species. This method provided valuable information regarding the kinetics of fly ash based geopolymers. It has one main limitation that is when alkaline solution contains excess silica for fly ash activation, the silicate species generate peaks at the same locations where the peaks due to geopolymer appear, so both peaks mix with each other, and it becomes very difficult to separate peaks due to silicate and geopolymer. Therefore, when silica is used in excess in alkaline solution, the functional group analysis cannot be used.

Four phases were detected in metakaolin based geopolymers by grid nanoindentation of the Young's modulus and hardness. These include a porous phase, a partially developed geopolymer gel, geopolymer gel, and unreacted metakaolin. The fractions of these phases in the final geopolymer depend on the chemical composition of raw material. The Na/Al and Si/Al ratios affected the reaction kinetics, geopolymer gels, and the mechanical properties of geopolymers.[79] The Si/Al ratio of 1.7 and Na/Al ratio of 0.9 were optimal for producing the best mechanical strength geopolymer. It was observed that silica enhanced the dissolution of metakaolin at Si/Al ratios below 2 : 1 and the formation of N-A-S-H gel depends on the dissolution of Al in case if silica is used as an alkaline activator.[80] This study provided good information about geopolymer gel formation

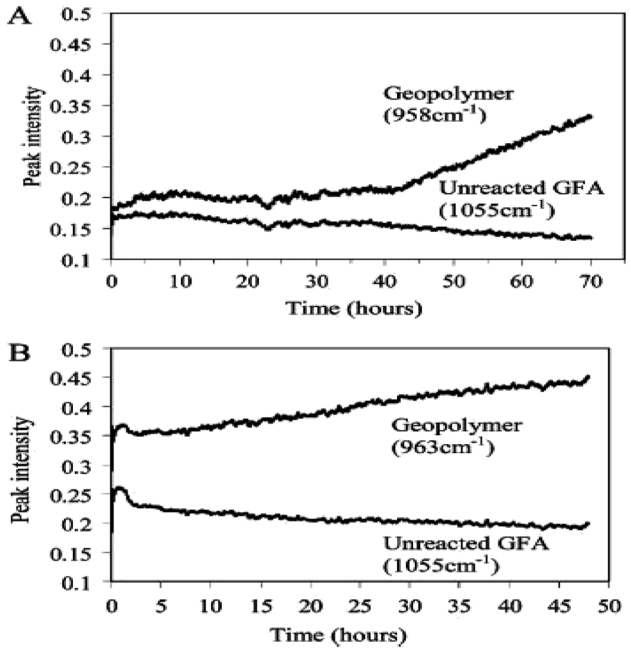

Fig. 3 Functional group analysis for geopolymer with (Na/Al = 0.5), (A) hydroxide activated and, (B) silicate-activated (SiO_2) = 2.5 M).[6]

and mechanical strength. This understanding combined with chemical composition of raw materials can be used to optimize the synthesis of geopolymers for higher mechanical properties.

The early age geopolymerization kinetics (up to first 72 hours) of metakaolin based geopolymer was determined mutually by using ^{1}H low-field Nuclear Magnetic Resonance (NMR) and Isothermal Conduction Calorimetry (ISC) at varying silicate moduli (SiO_2/Na_2O– 1, 1.2, 1.5, 1.8, and 2.0). The ^{1}H low-field NMR determined the state and relative amount of water in geopolymer paste and ISC determined the heat evolution during geopolymerization. The results showed that the geopolymerization increased at higher alkalinity of activator solution which was due to increase of degree of reaction with the increase of alkalinity of activator solution. It was also observed that the heat flow and cumulative heat release increased with the decrease of silica modulus of geopolymer due to fast dissolution of soluble species and higher quantity of formed product. The JMAK model was also used to determine the geopolymerization kinetics which described the kinetics of geopolymer prepared using numerous activators as a one-dimensional diffusion-controlled reaction and its rate of reaction slightly decreased at higher alkalinity due to the presence of various soluble species and more reaction products.[81] This method provided valuable information about geopolymerization kinetics, and it was proved that both techniques can be used mutually to determine the geopolymerization kinetics of metakaolin based geopolymers.

The structural evolution of metakaolin based geopolymer determined using Proton Nuclear Magnetic Resonance (^{1}H NMR) showed two relaxation peaks in the spin-lattice relaxation time (T1) during early 15 minutes of reaction. The first peak was due to filling of the water in the space between metakaolin particles and the second relaxation peak was due to the presence of water in flocculation structures. The increase of reaction time decreased the average mean value of T1. According to this study, the geopolymerization consists of four stages such as induction period, acceleration period, deceleration period, and stabilization period.[82] This method provided valuable information about the stages involved in the structural evolution of geopolymer. A new method of determination of reaction kinetics at early stages of geopolymerization based on evolution of internal Relative Humidity (RH) was developed. This method is like cumulative heat evolution in the Isothermal Conduction Calorimetry method, but it shows a higher signal to noise ratio specifically for geopolymers prepared using reactants of low reactivity. According to this method when the geopolymer is prepared using activator solution which contains waterglass, the reaction is mainly diffusion-controlled at higher temperature, and it changes from loose layer to a dense layer during the reaction time and if the activator solution is only NaOH solution then the reaction rate is mainly controlled by a diffusion layer through a dense layer at different temperatures. It was also noticed that the developed method is good for fly ash geopolymers when the degree of reaction of fly ash is below 0.35. This method can also be used for other raw materials with the consideration of possible self-desiccation.[83]

3.2 Phenomenological kinetics

It was observed that three processes control the geopolymer formation using modified Jandar model. The reactions include first order surface reaction between alkali hydroxide and glassy phase of fly ash particles, classical Fick diffusion through a surface layer, and a diffusive transport through a more complex gel structure (interstitial gel). The rate of reaction increased with the increase of KOH concentration (5–10 M), temperature (22–75 °C), and W/S ratio (0.35–40).[84] It was observed using exponential and Knudson linear dispersion models on the activation of blends of metakaolin, fly ash, and slag systems that the slag-based pastes exhibited features like Ordinary Portland Cement (OPC) which depended on the molarity of alkaline solution. The effect of temperature was higher on fly ash activation as compared to slag. Time parameter of both models showed similar effects with the increase of temperature but when compared to slag and ordinary Portland cement (OPC) pastes, the fly ash rich pastes showed reverse trend.[85] This study shared valuable information about the activation process of metakaolin, fly ash, and slag systems and the effects of temperature on model parameters but did not explain the overall geopolymerization reaction. A study determined the kinetics of fly ash geopolymer using John–Mehl–Avrami–Kolmogorov (JMAK) model and found that geopolymerization was a one dimensional diffusion controlled reaction which occurred through thickening of large product layers.[86]

The phenomenological models are helpful in describing the overall geopolymerization reaction, but it can be noticed that only a few studies have been conducted on the geopolymerization kinetics using phenomenological models while

more studies have been conducted using mechanistic tools. All studies provided new information about the geopolymerization kinetics of geopolymers with some techniques having few limitations in analyzing the kinetics such as Environmental Scanning Electron Microscopy (ESEM) and Energy Dispersive X-Ray Diffractometry (EDXRD) are only effective during the early setting period. The ATR-FTIR technique used to determine the geopolymer gel formation in a fly ash based geopolymer fails if the alkali solution contains excess silica. A modified Jandar model used to determine the geopolymerization kinetics best suits the systems containing particles of uniform size but fly ash contains particles of varying sizes. A method used to monitor the geopolymerization and reaction products formed in metakaolin based geopolymer using Isothermal Conduction Calorimetry (ICC) cannot be used for fly ash geopolymer system due to the unavailability of thermochemical parameters for fly ash geopolymers and without them the extent of geopolymerization cannot be quantified. These limitations need to be removed and new methods or techniques must be developed to overcome the limitations and get more detailed information about kinetics of all types of geopolymers. It has been observed that the mechanistic models provide more detailed information about geopolymerization kinetics and formation mechanism while phenomenological models only thoroughly describe the geopolymerization kinetics and formation mechanism. However, phenomenological models can also determine geopolymerization kinetics and formation mechanisms of such complex systems where mechanistic models cannot be used. Table 2 summarizes the studies conducted on the kinetics of geopolymerization along with their main findings.

4. Mechanisms of geopolymerization

The mechanism of geopolymer formation is crucial in understanding the reactions taking place and their sequence or order.

Table 2 List of studies conducted on kinetics of geopolymerization

S. no.	Type of geopolymer	Curing regime (hours)	Technique	Findings	Ref.
Mechanistic kinetics					
1	Metakaolin	4	ESEM	• Gel formation • The rate of reaction decreased with increase of silica	69
2	Metakaolin	3	EDXRD	• Na-geopolymer reacted rapidly compared to K-geopolymer	71
3	Metakaolin	72	ICC	• Four peaks detected due to dissolution, polymerization, and reorganization and crystallization of geopolymers	72
4	Metakaolin and slag	3072	X-ray PDF	• Extent of reaction was fast for silicate-activated geopolymers as compared to hydroxide activated metakaolin geopolymers. • Extent of reaction was fast for hydroxide activated as compared to silicate activated slag	76
5	Fly ash	72	ATR-FTIR	• Induction period • Si–O-T peak unaffected after 72 hours	6
6	Aluminosilicate source materials	100	ICP-OES	• Silicate sources dissolve rapidly as compared to aluminosilicate sources • Dissolution rate of fly ash was higher • Increase of molarity increased dissolution rate up to some point • Milling resulted in the increase of release of Si in fly ash and Al in GBFS	91
7	Metakaolin	72	^{1}H low-field NMR and ISC	• Geopolymerization is a one-dimensional diffusion-controlled reaction • The high alkalinity enhanced the geopolymerization, gel formation, and growth rate due to the presence of various soluble species and more reaction products	81
8	Fly ash	168	Relative humidity (RH)	• For water glass activated geopolymers, the reaction rate is diffusion controlled which changes from a loose layer to a dense layer. • For NaOH activated geopolymers, the rate of reaction is diffusion controlled through a dense layer at different temperatures	83
Phenomenological kinetics					
9	Fly ash	168	JMAK	• Geopolymerization is a one-dimensional diffusion-controlled reaction, and it grows in the form of thickening of large product layers	86
10	Fly ash	672	Modified Jandar model	• A first order surface reaction, classical Fick diffusion, and a diffusive transport through a more complex gel structure • The reaction rate increased with the increase of KOH concentration, temperature, and W/S ratio	84

The mechanism of geopolymerization depends on aluminosilicate source materials and alkaline activator.

Many mechanisms have been proposed for geopolymer formation. Glukhovsky (1980) described the mechanism of geopolymerization consisting of two steps; breaking of raw materials and condensation of the produced product.[87] The destruction or breaking of raw materials is carried out by breaking of covalent bonds between Al–O–Si and Si–O–Si using alkaline solution which produces a colloidal phase. Then coagulation occurs which joins destroyed products and finally produces a condensed structure. Some other studies also proposed similar mechanisms consisting of silica dissolution, transportation, and polycondensation reactions.[88,89] All these steps occur simultaneously and it is very difficult to separate these steps.[90] Davidovits (1988) described geopolymerization as an exothermic reaction that is conducted through oligomers (dimer, trimer) which produce structural units for three dimensional arrangement.[92] It consists of the reaction of aluminosilicate oxides with alkalis and alkali-polysilicates which produces polymeric Si–O–Al bonds having $(SiO_2, Al_2O_3)_n$ formula. Another study described mechanism consisting of dissolution of solid aluminosilicate oxides by alkali solution, movement of the dissolved silica and alumina from particle surface to interparticle space, development of gel phase, and hardening of the gel phase.[93] The reaction sequence is given below,

$$\text{Al–Si material (s)} + \text{MOH (aq)} + Na_2SiO_3\ \text{(s or aq)} \quad (1)$$

$$\rightarrow \text{Al–Si material (s)} + [M_z(AlO_2)_x(SiO_2)_y \cdot n\text{MOH} \cdot mH_2O]\ \text{gel} \quad (2)$$

$$\rightarrow \text{Al–Si material (s)}\ [M_a((AlO_2)_a(SiO_2)_b) \cdot n\text{MOH} \cdot mH_2O]\ \text{gel} \quad (3)$$

The quantity of Al–Si material used in reaction (1) and (2) depends on the particle size, dissolution of Al–Si, and alkaline solution concentration. The amount of gel produced in reaction (2) depends on the dissolution of Al and Si while the amorphous geopolymer is formed in reaction (3). The time required to produce a geopolymer gel depends on the processing conditions.[94] A study developed two mechanism models, one for alkali activation of blast furnace slag (Si + Ca) using mild alkaline solution with CSH as the final product and another for activation of aluminosilicate (Si + Al) generally metakaolin using alkaline solution from mild to high.[90] The former model is like a zeolite formation which shows that the alkali activation of metakaolin produces amorphous polymers like zeolites. In another mechanism study, a delay or induction was noticed after dissolution of raw materials in sodium hydroxide activated metakaolin geopolymer while no induction period was detected in sodium silicate activated metakaolin and dissolution was followed by fast polycondensation reaction.[95]

Three calorimetric peaks due to dissolution of metakaolin, induction period, and final structure formation were detected in sodium hydroxide activated metakaolin based geopolymer using ISC as shown in Fig. 4.[96] It shows three peaks of metakaolin based geopolymers activated using different concentrations of sodium hydroxide (5–18 M). The peaks were different for geopolymers activated using NaOH concentration of 5 M and those with NaOH concentration of ≥10 M. In the case of geopolymers activated using NaOH concentration of ≥10 M, the intense signal showed the precipitation of reaction products, and these occur at similar activation times. The samples activated using 5 M NaOH solution showed weak calorimetric signal with lower intensity. The hydration process of blast furnace slag based geopolymer depends on the content of sodium and silica modulus (M_s). The heat of hydration increased with the increase of sodium content and silica modulus. Geopolymerization started with the destruction of bonds between slag atoms such as Si–O–Si, Al–O–Al, Al–O–Si, Ca–O, and Mg–O, which was described by the initial heat release peak and the formation of Si–Al layer on the surface of slag grains was described by the appearance of a new peak. Then finally, the hydration product started to form.[97] Some other studies also described geopolymer formation mechanism as consisting of three steps.[98,99] It has been observed that the water is used during dissolution of source materials while it is released during polymerization. A mechanism study found that the activation of fly ash by alkali follows the same steps involved in the formation of different types of zeolites and forms alkaline aluminosilicate as the product.[100] The alkali activation of aluminosilicate produces a nucleation phase. When nuclei reach a critical size, it starts crystallization that is a slow process and a long-time crystalline product form. The increase of SiO_2/Al_2O_3 ratio decreased the initial reaction rate.[71,101] It was observed that the initial phase produced later transformed to a more ordered phase during geopolymerization.

A new reaction sequence which is an extension of the Faimon (1996)[102] model was proposed as shown in Fig. 5.[101,103] According to this model, aluminosilicate source material dissolves to produce aluminate (A) and silicate (S) monomers, which then form aluminosilicate oligomer (O). Oligomers polymerize to produce aluminosilicate polymer (P) and aluminosilicate nuclei (N-quasi or nano-crystalline). The aluminosilicate polymer transforms to aluminosilicate gel (G-amorphous) while aluminosilicate nuclei transform to zeolitic phases (Z-crystalline). The formation of a primary Al rich gel in

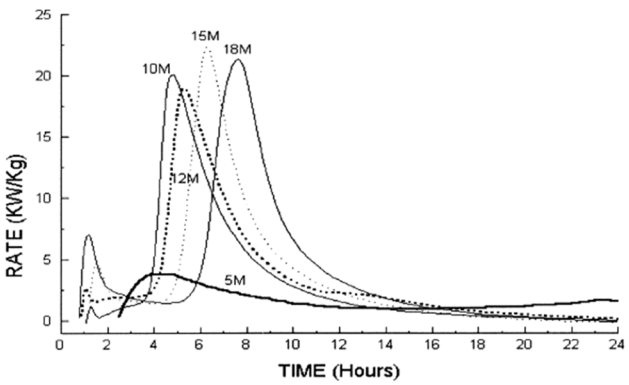

Fig. 4 Calorimetric curves of geopolymers activated using different concentrations of NaOH, MK/$Ca(OH)_2$ ratio of 1 : 1 and temperature of 45 °C.[96]

hydroxide activated fly ash geopolymer was observed. The Al released passivated the surface of fly ash and further fly ash dissolution stopped causing a delay or induction in the process. Induction period was not detected in the systems when seeding and sodium silicate were used. During the delay period, Al-rich gel established pseudo equilibrium through depolymerization/repolymerization reactions with the surrounding solution. Gel nuclei began to form in Si-rich gel and then the growth of a new phase started. The strength development and durability of geopolymers depend on this new phase.[104]

The nucleation of the gels, reorganization, and polymerization was observed at 60 °C in high calcium fly ash based geopolymers by analyzing geopolymerization reaction using Quasielastic neutron scattering (QENS). The geopolymers synthesized using 14 M NaOH solution contained higher quantity of chemically bound water as compared to geopolymers synthesized using 10 M NaOH. The concentration of NaOH and temperature played main roles in the initial gel formation and polymerization at later stages.[105] The mechanism of geopolymerization of phosphoric acid based geopolymer consisted of three steps such as removal of aluminum from metakaolinite, the reaction between tetrahedral PO_4 and –Si–O– layer to form amorphous (–Si–O–P–) structure and the reaction of aluminum with PO_4 tetrahedra to form crystalline $AlPO_4$, and the condensation of the amorphous phase to form a geopolymer.[106] The addition of graphene (rGO) in metakaolin geopolymer decreased the voids with the increase of geopolymerization time. The degree of amorphicity of metakaolin based geopolymer also decreased with the increase of reaction time. The five and six coordinates of Al–O sites were converted into four coordinates with the addition of graphene. The structure of metakaolin geopolymer consisted of Si in the form of Q_4 (3Al). The graphene (rGO) bonded with the geopolymer reaction products and increased the density of the geopolymer matrix.[107]

Another reaction model for the mechanism of geopolymerization is shown in Fig. 6. The geopolymerization starts by dissolving aluminosilicate with the help of alkali solution which releases aluminate and silicate species into the solution. Aluminate and silicate species and the silicate in alkaline solution forms a complex mixture consisting of aluminate, silicate, and aluminosilicate species and the speciation equilibrium develops in the solution. The dissolution of amorphous aluminosilicate source material at high pH is quick and forms a supersaturated aluminosilicate solution. In the case of concentrated solution, it results in the formation of gel by the condensation of oligomers which release water. The time required for the formation of a gel depends on raw materials, solution composition, processing conditions, and synthesis conditions.[108] It has been observed that some systems never form gel due to dilute nature and the concentration of alumina and silica varies because of the slow response of the system which is far away from equilibrium.[102] The system continues to rearrange and reorganize after gel formation resulting in the formation of a three-dimensional aluminosilicate network. Nucleation develops in the second gel and growth is the condition in which nuclei reaches a critical size and crystals start to form.

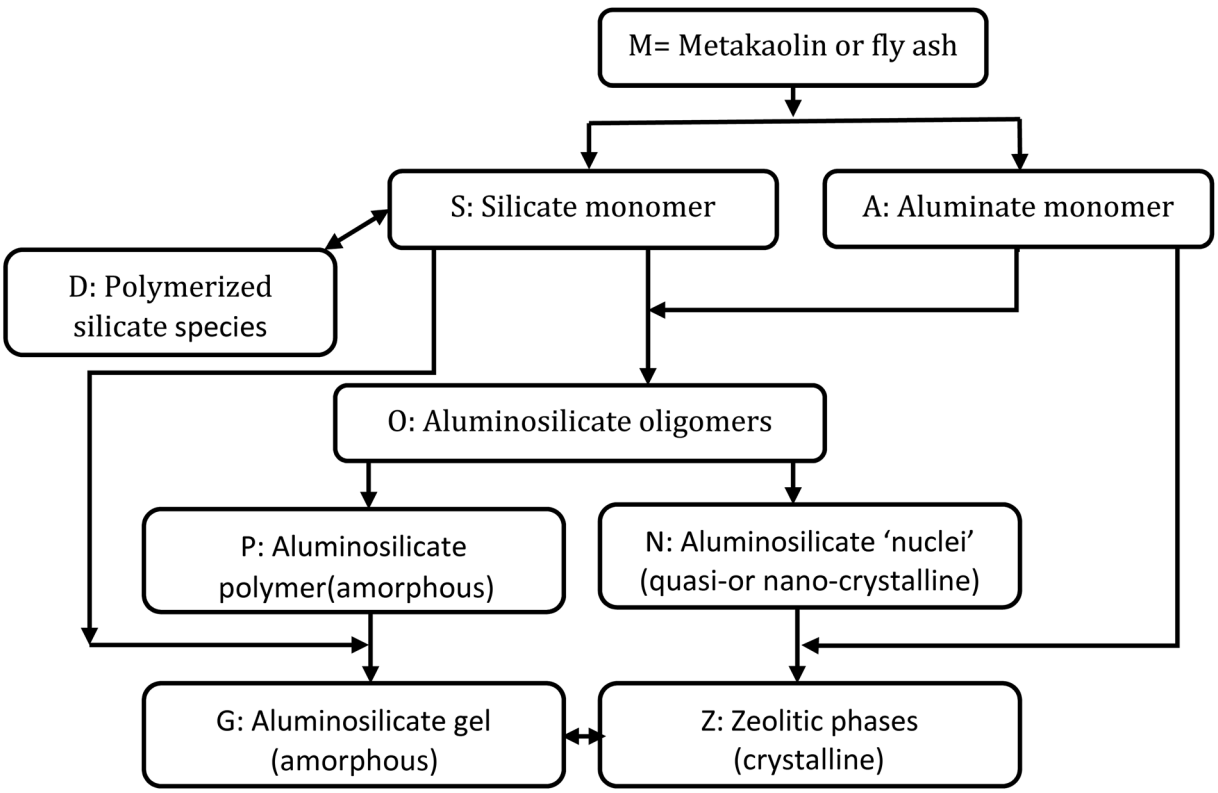

Fig. 5 Proposed reaction sequence of geopolymerization.[101,103]

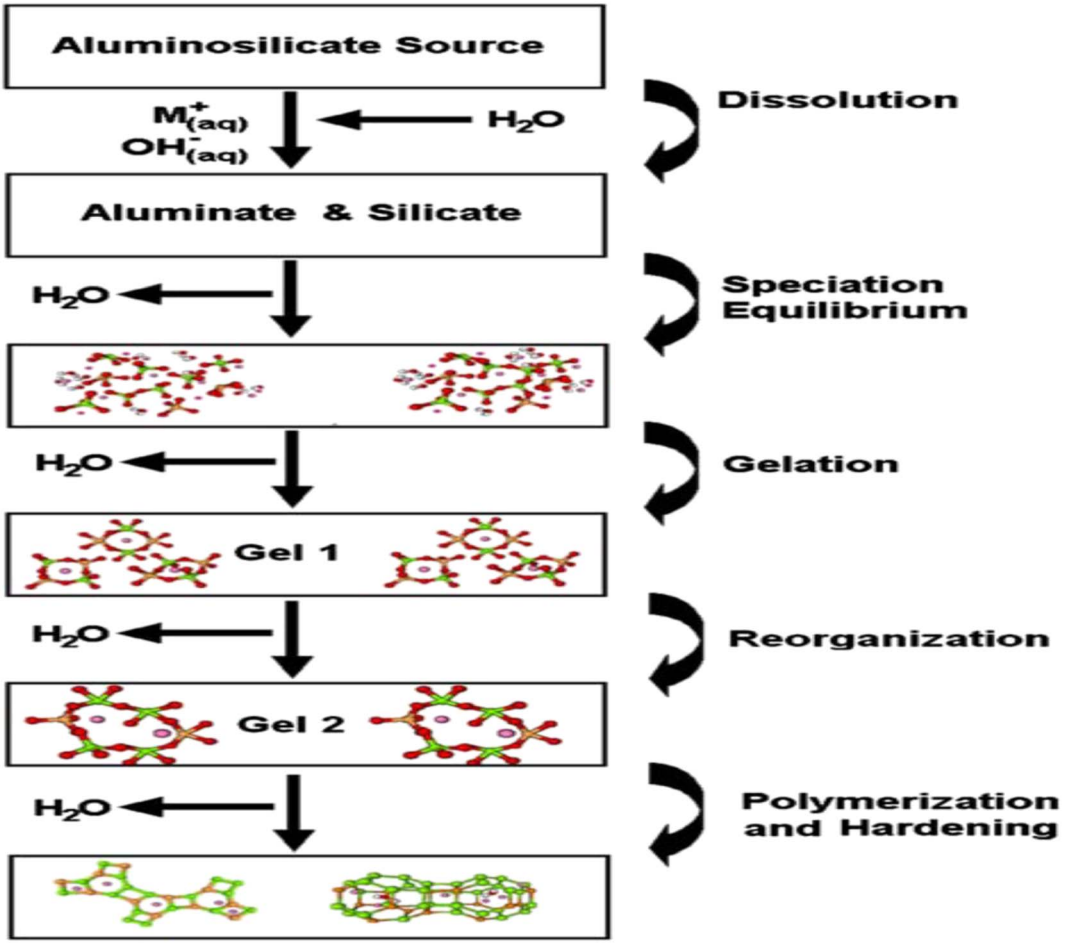

Fig. 6 Model for mechanism of geopolymerization.[4]

The early stage geopolymerization mechanism of metakaolin based geopolymer determined using Magnetic Resonance Spectroscopy (NMR) based on vacuum dehydration technique by fuzzy analysis of deconvolution data found that the mechanism consists of four stages, (i) dissolution of raw materials to produce monomers, (ii) nucleation free polymerization, (iii) structural rearrangement-collapse and rearrangement through loss of free water, and (iv) unordered condensation or repolymerization in flaw sites.[109] It is a good technique as it provides quantitative and qualitative data. This finding supports the geopolymerization mechanism described by Duxson *et al.*[110] A study determined the synthesis mechanism of phosphate based metakaolin geopolymer using various tools such as *in situ* quasi-isothermal Differential Scanning Calorimetry (DSC), Atomic Absorption, pH meter, Magic Angle Spinning Nuclear Magnetic Resonance (MAS-NMR), Scanning Electron Microscopy (SEM) with Energy Dispersive X-ray (EDX) analysis, and Fourier Transform Infrared Spectroscopy (FTIR). It was observed that the amorphous structure of geopolymer consists of –Si–O–Al–O–P– units with some –Si–O–P terminal units. The formation mechanism consisted of three steps. The first step is dealumination which occurs during the first 30 minutes of reaction. It consists of two elementary steps such as dealumination of total –Al–O–Al bonds and the second one is partial which concerns the dealumination of –Si–O–Al bonds. The second step is condensation which consists of four stages according to the chemical composition of reactant and obtained product. The four stages of condensation include the formation of silicate aluminum phosphate phases, aluminum phosphate phases, silicate phosphate phases, and amorphous silica phases. It occurs during the initial reaction time of 12 hours with varying speed which decreases with the reaction time and becomes constant after 12 hours. The polycondensation which is the third step starts during first hour of reaction and continues slowly up to many days and results in the 3D polymerized network.[111] This study provided valuable information on the synthesis mechanism of phosphate based metakaolin geopolymer which can be extended by using other activator solutions.

A study determined the effect of milling time of fly ash of 0, 30, and 90 minutes on the geopolymerization kinetics and mechanism using Isothermal Conduction Calorimeter (ISC). The apparent activation energy decreased with the increase of milling time due to the increase of reactivity of fine particles. The effect of fly ash particle size was more at low reaction temperature while only small effect in peak amplitude and

required time to reach was observed at higher temperature. There was no effect of particle size of fly ash on the early age geopolymerization mechanism which occurred by nucleation and growth. The reaction rate and activation energy were affected by fineness of fly ash particles. The rate of geopolymerization increased with the increase of fineness of fly ash particles. The activation energy determined by rate method showed three stages of geopolymerization consisting of dissolution, gelation, and restructuring. The geopolymerizatiom mechanism was unaffected by the change of reaction temperature in the range of 39–55 °C.[112] This study provided very good information about the effect of milling of fly ash and milling time on the geopolymerization kinetics and mechanism using ISC technique.

A summary of the geopolymerization mechanism is given in Table 3. The studies conducted to determine the geopolymerization mechanism provided new information and some studies verified the existing information about geopolymerization mechanism. According to the literature analysis, the geopolymerization mechanism consists of three to four stages depending on the type of aluminosilicate and type of alkali.

5. Effect of parameters on geopolymerization

The parameters such as silica to alumina (Si/Al) ratio, sodium to alumina (Na/Al) ratio, water to solid (W/S) ratio, and temperature affect the geopolymerization kinetics.

5.1 Silica to alumina (Si/Al) ratio

The synthesis of geopolymer gel with strong inter-particle bonding and higher mechanical strength requires the use of silica. At Si/Al ratio of 1, the condensation between aluminate and silicate species produced poly(sialate) polymer structure, and at Si/Al >1, the silicate species produced by hydrolysis of SiO_2 condensed among themselves and produced oligomeric silicates and the oligomeric silicates condensed with $Al(OH)_4^{4-}$ and produced 3D network of polymer structures consisting of poly (sialate-siloxo) and poly (sialate-disiloxo).[114] It has been noticed that the higher Si/Al ratio (~1.7) increases the number of Si–O–Si bonds and the amount of geopolymer gel.[79] It has been observed that the low Si/Al ratio increases the number of tetrahedral Al incorporating into the silicate backbone whereas increase in Si/Al ratio increases the compressive strength, but the increase of Si/Al ratio above a certain point (>1.7) increases the pore size and produces fast setting and low compressive strength geopolymers. Another study observed that the increase of SiO_2/Al_2O_3 ratio from 2.0 to 4.0 increased the initial rate of reaction but higher SiO_2/Al_2O_3 ratio caused solidification of the paste prior to completion of reaction.[71] The use of highly reactive silica increased the gel formation and compressive strength of geopolymer.[115] The Si/Al ratio of the specimen can be used to predict the resonance position and shape of geopolymers using ^{29}Si MAS NMR.[116,117] The Si/Al ratio depends on the raw materials composition, and it should be kept above the Si/Al ratio of the raw material to produce a higher compressive strength geopolymer.

5.2 Molarity of alkali solution

The concentration of alkali solution is a very important parameter for geopolymerization.[118] Potassium hydroxide (KOH) releases higher amount of alumina and silica as compared to NaOH.[119,120] The solubility of aluminosilicate material increases with the increase of concentration of hydroxide ions.[121] The higher Na/Al ratio speeds up the dissolution and polymerization reactions and it also increases the amount of geopolymer gel but the Na/Al ratio of 1.2 decreases the compressive strength at later ages (28 days). It has been observed that the increase of Na/Al ratio from 0.74 to 1.10 increased the reaction rate.[72] The excessive concentration of OH^- results in the decrease of the strength of geopolymer.[90] The higher alkalinity of hydration water results in a decrease in rate of hydration. By increasing the activator concentration, a delay in the polymer formation was observed and the concentration of ionic species also increased which decreased the mobility of ions and delayed the formation of coagulated structures.[122] The

Table 3 A summary of geopolymerization mechanisms described in literature

Raw material	Description	Ref.
Metakaolin	Dissolution, induction, and polycondensation (hydroxide activated) Dissolution and polycondensation (sodium silicate activated)	95
Blast furnace slag	Destruction of raw materials, formation of Si–Al layer, and formation of geopolymer	97
Fly ash and kaolinite	Dissolution, orientation of dissolved species, and condensation and hardening of structure	98
Kaolin and sodium and potassium feldspar	Dissolution, polymerization, and condensation	113
Metakaolin and fly ash	Dissolution, polymerization, and gelation	101 and 103
Fly ash	Dissolution, nucleation phase, crystallization	100
Metakaolinite	Dissolution of aluminum, reaction between tetrahedral PO_4 and –Si–O– to form –Si–O–P– structure and reaction of aluminium with PO_4 tetrahedra to form crystalline $AlPO_4$, and condensation	106

increase of alkali concentration from 5 to 10 M in a fly ash based geopolymer produced an amorphous geopolymer with a small amount of CSH gel. The increase of Na/Al ratio up to 0.63 increased the rate of reaction while further increase in this ratio decreased the rate of reaction.[6] The aluminosilicate gel as the main product and the CSH gel as the secondary product were obtained in case of metakaolin activated with highly concentrated alkali solution in the presence of calcium.[122] The use of higher content of calcium in the geopolymer system results in the formation of some form of CSH gel. The higher content of Na also increases the formation of CSH gel. At a higher content of Na, less calcium will be available to react with aluminate and silicate species and will precipitate out as the CSH gel. It is still not clear that calcium participates like sodium or potassium in the geopolymer formation or not.[123] It has been observed that CSH gel fills the gaps and voids available in the geopolymer and increases the mechanical strength of the produced geopolymer.[124]

5.3 Silica modulus (SiO_2/M_2O)

The ratio of silicate to hydroxide plays an important role in the rate of reaction and the development of compressive strength of geopolymers. The increase of concentration of alkali M_2O (M–Na/K) or decrease in the concentration of added SiO_2 increases the compressive strength of geopolymers.[13] This is because excess sodium silicate hinders the evaporation of water as well as the formation of the structure of geopolymer. The system activated with sodium silicate and sodium hydroxide possessed higher compressive strength while the system activated with potassium silicate and potassium hydroxide and potassium silicate and sodium hydroxide were weak.[125–127] K^+ is more basic which causes higher dissolution and polycondensation reactions and higher network formation resulting in higher compressive strength geopolymers.[53] The large size of K^+ also favors polycondensation reactions.[128,129] It has been noticed that silica modulus in case of sodium silicate equal to or higher than 0.8 produces amorphous geopolymer and silica modulus below 0.8 produces semi-crystalline geopolymers.[130] A study on the effect of silica modulus (0.424–1.716) on the geopolymerization of natural pozzolan based geopolymer through Isothermal Conduction Calorimetry (ICC) found that the early-stage dissolution of aluminate and silicate species depends on the molar contents of SiO_2 and Na_2O. The increase of silica modulus decreases the degree of reaction but decrease of silica modulus below certain point decreases the compressive strength of geopolymer. Very low and very high silica modulus are not good for compressive strength and results in the decrease of compressive strength. It was also observed that the participation of the various crystalline and amorphous phases of raw materials in the geopolymerization reaction also depends on the content of silica modulus. It was also noticed that the low silica modulus results in the efflorescence which cause decrease of compressive strength of geopolymer while higher silica modulus again reduces compressive strength due to lower degree of reaction.[131]

5.4 Water/solid (W/S) ratio

Water is an important parameter which affects the rate of reaction and compressive strength of geopolymers. Water content of the activator is also significant along with the speciation and silicate concentration of the activator.[130] Water is involved in the dissolution, polycondensation, and hardening stages of geopolymerization. The amount of water should be selected in a way that geopolymerization completes all its stages as well as the workability of the paste is sustained. The amount of water required for the synthesis of geopolymers depends on the type of aluminosilicate and the shaping method used such as molding, pressing, and extrusion.[132] The effect of water content on the synthesis of geopolymer is determined through water to solid (W/S) ratio or solid to liquid (S/L) ratio. The increase of W/S ratio by mass decreases the strength of geopolymers and the same trend has also been observed in the formation of Ordinary Portland Cement (OPC). The W/S ratio of 0.4 is the minimum ratio in the case of Portland cement and the same ratio is also possible in geopolymers. L/S ratio from 0.30 to 0.45 has been recommended for the synthesis of geopolymers.[133] The water content of geopolymers is approximately 10% less as compared to water content of zeolites.[98]

The effect of S/L ratio on the geopolymerization kinetics of class C fly ash geopolymer was determined using John–Mehl–Avrami–Kolmogorov (JMAK) model through heat evolution measured by Differential Scanning Calorimeter (DSC). The variation of S/L ratio affected the heat evolution and growth of geopolymers. The Avrami exponent (n) was in the range of 0.942–1.2045, which showed that the geopolymer growth during setting was governed by one-dimensional heterogeneous nucleation with rod-like growth. The nucleation was heterogeneous because it involved the transformation of liquid and solid phases and it was an instantaneous growth which occurred in available nucleation sites of monomers and it has been noticed in literature that the nuclei form on the surface of foreign particles in heterogenous nucleation.[134] The increase of S/L ratio to 2.5 increased the value of n due to the increase of the nucleation sites. The value of n was below 1 at S/L ratios of 1 and 3 due to the slow nuclei growth and it is against JMAK model assumptions. The geopolymer growth was slow at S/L ratio of 1 due to a smaller number of nucleation sites because of the presence of higher concentration of OH^- ions and it resulted in the improper geopolymer growth and at S/L ratio of 3, the geopolymer growth hindered due to presence of higher number of unreacted fly ash particles. The increase of S/L ratio up to 2.5 increased the growth rate (k) while further increase up to 3 slightly decreased the growth rate (k). The decrease in growth rate was due to compactness of fly ash particles at the minimum alkali which resulted in the decrease of growth rate.[135]

5.5 Curing conditions

Curing time and curing temperature affect the kinetics of geopolymerization and mechanical strength of geopolymers. The reaction temperature and curing time are very important for determining the structure of the final product.[4]

• Curing time

The curing time from 2 to 5 hours is very important and the temperature curing of geopolymers up to 24 hours increases the compressive strength of geopolymers while further curing increases the compressive strength very slowly due to alkaline saturation and product densification.[13] A study found that geopolymer achieved compressive strength of 65 MPa in 24 hours while further strength development was insignificant.[136] Another study found that the geopolymers cured at 65 °C produced higher compressive strength in early 24 hours while the geopolymers cured at 25 °C produced higher compressive strength at later ages.[118] The compressive strength of geopolymers is directly proportional to the amount of geopolymer, higher the geopolymer formation, the higher is the compressive strength and *vice versa*. For kinetics studies, the curing time depends on the interest of the phase of study.

• Curing temperature

There are three methods of curing geopolymers such as vapor-proof membrane curing, temperature curing (TC), and wet curing (WC). Temperature is involved in the setting of the paste and concrete and it accelerates the geopolymerization reaction. The reaction of fly ash is very slow at room temperature which makes it unfeasible due to delayed setting while it can be avoided by processing at elevated temperature.[137,138] It has been observed that the low temperature curing of geopolymer is not suitable for development of mechanically strong geopolymers.[139] It has been noticed that heat curing is good for strength gain in geopolymer as compared to curing at room temperature (strength obtained after 24 hours of elevated temperature curing is equal to the 1 month of curing at ambient temperature).[140] Elevated temperature curing at the start of reaction catalyzes the formation chemistry in an appropriate way.[141] The temperature curing of geopolymer for 24 hours is best especially for practical applications.[133]

There are two types of temperature curing, open curing, and closed curing. It has been observed that open curing results in the evaporation of water which results in the decrease of amount of alkaline solution available for the reaction and causes precipitation of the alkali salt. This condition results in a decrease of strength and increases the porosity of the material. The geopolymer cured in closed conditions possess lower porosity and higher binding matrices and it is suitable for immobilization of the heavy metals and other hazardous wastes.[142] The higher reaction temperature and higher surface area of aluminosilicate material increases the extent of reaction. Temperature also increases the crystallinity of geopolymers.[143] The effect of increase of temperature is more on the reaction kinetics as compared to the effect of increase of activator concentration.[144] It has been observed that the temperature in the range of 65–80 °C improved the mechanical properties of sodium hydroxide activated fly ash geopolymers.[140,145,146] The curing of Na-based geopolymer at high temperature caused faster dissolution and faster gel growth due to coagulating ability of Na^+ with monomeric silicate species which causes faster setting.[147,148] While in case of K-based geopolymer, the higher temperature will not allow gelation step to proceed unless there is a sufficient amount of nutrients (larger aluminosilicate anions) for gel growth.[148]

The optimum Si/Al ratio depends on the raw materials used for the synthesis of geopolymers. The Si/Al ratio a little bit above the Si/Al ratio of reactants enhances the degree of reaction and compressive strength of geopolymers. The Na/Al ratio of 1 is normally used for the synthesis of geopolymers. The water to solid (W/S) ratio of 0.30–0.45 is recommended for the synthesis of geopolymers. A curing time of 24 hours is the best for geopolymers. The normal range of temperature used for curing of geopolymer is from 30 °C to 85 °C.[90,149,150] There is an upper limit above which further increase in temperature decreases the production of geopolymers and most of the raw material remains unreacted and compressive strength decreases due to fast setting and decrease of workability of paste.[151]

6. Conclusions and future perspectives for kinetics and mechanism of geopolymers

The research on kinetics and mechanisms of geopolymerization is developing the understanding of the reactions involved and the formation mechanism of geopolymers. The brief conclusions and future perspectives are given below,

1. Fly ash, metakaolin, and GGBFS are commonly used for synthesis of geopolymers while a variety of new materials such as red mud, palm oil fuel ash, bottom ash, clays, volcanic ash, bagasse bottom ash, loess powder, iron ore tailings, and gold mine wastes *etc.* are being introduced as raw materials for the synthesis of geopolymers.

2. Attenuated Total Reflectance-Fourier Transform Infrared Spectroscopy (ATR-FTIR), Isothermal Conduction Calorimetry (ICC), Environmental Scanning Electron Microscopy (ESEM), Energy Dispersive X-Ray Diffraction (EDXRD), X-Ray Pair Distribution Function (PDF) analysis, ^{1}H low-field Nuclear Magnetic Resonance (NMR), John–Mehl–Avrami–Kolmogorov (JMAK) model, and modified Jandar model used for geopolymerization kinetics provided valuable information and developed the understanding of geopolymers but each of these techniques possess some limitations.

3. Many models have been proposed for the mechanism of geopolymerization describing geopolymerization mechanism consisting of 3 to 4 stages which involves dissolution, polymerization, condensation, and reorganization.

4. The parameters such as Si/Al ratio, Na/Al ratio, W/S ratio, SiO_2/M_2O ratio, curing time, and curing temperature affect the geopolymerization of aluminosilicate source materials and their effect depends on the raw materials.

5. New mechanistic and phenomenological approaches should be developed for further understanding of the kinetics and mechanism of geopolymers prepared using new types of aluminosilicate source materials.

6. New mechanistic and phenomenological techniques applicable for all types of geopolymers must be developed.

7. New advanced techniques need to be developed for determining the chemical formula of geopolymers.

8. Advanced numerical modeling tools should be used for studying the geopolymerization kinetics and formation mechanism of geopolymers.

Author contributions

Ahmer Ali Siyal: methodology and original draft preparation. Radin Maya Saphira Mohamed Radin: supervision and resources. Rashid Shamsuddin: writing – review & editing. Mohd Baharudin Bin Ridzuan: writing – review and editing.

Conflicts of interest

There are no conflicts to declare.

Acknowledgements

Authors are very thankful to Universiti Tun Hussein Onn Malaysia (UTHM) for offering Post-Doctoral Fellowship and supporting this research through the grant TIER 1 Q538.

References

1 C. Woolard, K. Petrus and M. Van der Horst, *Water SA*, 2000, **26**, 531–536.
2 V. D. Glukhovsky, Ancient, modern and future concretes, in *Proceedings of the First International Conference on Alkaline Cements and Concretes*, 1994, pp. 1–9.
3 M. Juenger, F. Winnefeld, J. Provis and J. Ideker, *Cem. Concr. Res.*, 2011, **41**, 1232–1243.
4 P. Duxson, A. Fernández-Jiménez, J. Provis, G. Lukey, A. Palomo and J. Van Deventer, *J. Mater. Sci.*, 2007, **42**, 2917–2933.
5 M. Ahmaruzzaman, *Prog. Energy Combust. Sci.*, 2010, **36**, 327–363.
6 C. A. Rees, J. L. Provis, G. C. Lukey and J. S. van Deventer, *Langmuir*, 2007, **23**, 9076–9082.
7 H. Yang, F. Dai, H. Chen, Y. He, Z. Wang and R. Wang, *J. Environ. Chem. Eng.*, 2023, **11**, 109481.
8 D. Hardjito, D. M. Sumajouw, S. Wallah and B. Rangan, *Aust. J. Struct. Eng.*, 2005, **6**, 77.
9 A. Palomo, M. Blanco-Varela, M. Granizo, F. Puertas, T. Vazquez and M. Grutzeck, *Cem. Concr. Res.*, 1999, **29**, 997–1004.
10 D. C. Comrie and W. M. Kriven, *Advances in Ceramic Matrix Composites IX*, 2012, vol. 153, pp. 211–225.
11 H. Chen, H. Yan, P. Cao, Y. He, P. Song and R. Wang, *New J. Chem.*, 2022, **46**, 18839–18847.
12 Z. Zhang, X. Yao and H. Zhu, *Appl. Clay Sci.c*, 2010, **49**, 1–6.
13 D. Khale and R. Chaudhary, *J. Mater. Sci.*, 2007, **42**, 729–746.
14 T. Guo, G. Zhang, F. Ma, P. Shen, R. Wang, W. Song, L. Wang, P. Han and X. Bai, *J. Build. Eng.*, 2023, **79**, 107789.
15 L. F. Fan, D. K. Chen and W. L. Zhong, *Constr. Build. Mater.*, 2023, **406**, 133391.
16 A. A. Siyal, M. R. Shamsuddin, N. E. Rabat, M. Zulfiqar, Z. Man and A. Low, *J. Cleaner Prod.*, 2019, **229**, 232–243.
17 A. A. Siyal, M. R. Shamsuddin, S. H. Khahro, A. Low and M. Ayoub, *J. Environ. Chem. Eng.*, 2021, **9**, 104949.
18 Q. Tian, C. Chen, M. Wang, B. Guo, H. Zhang and K. Sasaki, *Environ. Pollut.*, 2021, **274**, 116509.
19 J. Liu, G. Xie, Z. Wang, Z. Li, X. Fan, H. Jin, W. Zhang, F. Xing and L. Tang, *J. Environ. Manage.*, 2023, **341**, 118053.
20 M. Irfan Khan, K. Azizli, S. Sufian and Z. Man, *Ceram. Int.*, 2015, **41**, 2794–2805.
21 N. Yang, C. S. Das, X. Xue, W. Li and J.-G. Dai, *Constr. Build. Mater.*, 2022, **342**, 127942.
22 R. M. Hamidi, A. A. Siyal, T. Luukkonen, R. M. Shamsuddin and M. Moniruzzaman, *RSC Adv.*, 2022, **12**, 33187–33199.
23 H. Yang, F. Dai, Y. He and R. Wang, *Sustainable Chem. Pharm.*, 2023, **36**, 101250.
24 H. Yan, X. Zhu, F. Dai, Y. He, X. Jing, P. Song and R. Wang, *Colloids Surf., A*, 2021, **631**, 127646.
25 R. F. Botti, M. D. M. Innocentini, T. A. Faleiros, M. F. Mello, D. L. Flumignan, L. K. Santos, G. Franchin and P. Colombo, *Appl. Mater. Today*, 2021, **23**, 101022.
26 J. Upadhyay, S. P. Misra, S. Irusta, S. Sharma and P. A. Deshpande, *Mol. Catal.*, 2023, **536**, 112911.
27 A. L. Freire, C. D. Moura-Nickel, G. Scaratti, A. De Rossi, M. H. Araújo, A. De Noni Júnior, A. E. Rodrigues, E. R. Castellón and R. de Fátima Peralta Muniz Moreira, *J. Cleaner Prod.*, 2020, **273**, 122917.
28 S. Chang, Y. He, Y. Li and X. Cui, *J. Cleaner Prod.*, 2021, **316**, 128163.
29 E. Mittemeijer, *Fundamentals of Materials Science*, Springer Verlag, Heidelberg, 2010.
30 Y.-M. Liew, C.-Y. Heah and H. Kamarudin, *Prog. Mater. Sci.*, 2016, **83**, 595–629.
31 J. Liu, J.-H. Doh, D. E. L. Ong, Z. Liu and M. N. S. Hadi, *Constr. Build. Mater.*, 2023, **362**, 129784.
32 M. Zribi and S. Baklouti, *Polym. Bull.*, 2022, **79**, 6827–6855.
33 P. N. Lemougna, K.-t. Wang, Q. Tang, U. C. Melo and X.-m. Cui, *Ceram. Int.*, 2016, **42**, 15142–15159.
34 R. Blissett and N. Rowson, *Fuel*, 2012, **97**, 1–23.
35 M. Tiwari, S. Sahu, R. Bhangare, P. Ajmal and G. Pandit, *Appl. Radiat. Isot.*, 2014, **90**, 53–57.
36 S. V. Vassilev and C. G. Vassileva, *Fuel*, 2007, **86**, 1490–1512.
37 A. Committee, *Annual Book of ASTM Standard, Section*, 2004, vol. 4.
38 E. Moulin, P. Blanc and D. Sorrentino, *Cem. Concr. Compos.*, 2001, **23**, 463–469.
39 C. Nkoumbou, A. Njoya, D. Njoya, C. Grosbois, D. Njopwouo, J. Yvon and F. Martin, *Appl. Clay Sci.*, 2009, **43**, 118–124.
40 J. Kostuch, V. Walters and T. Jones, *Concrete*, 2000, **2**, 1799–1811.
41 P. Barnes and J. Bensted, *Structure and Performance of Cements*, CRC Press, 2002.
42 J. V. S. Metekong, C. R. Kaze, A. Adesina, J. G. D. Nemaleu, J. N. Y. Djobo, P. N. Lemougna, T. Alomayri, E. Kamseu, U. C. Melo and T. T. Tatietse, *Silicon*, 2022, **14**, 7399–7416.
43 R. García, R. V. de la Villa, I. Vegas, M. Frías and M. S. de Rojas, *Constr. Build. Mater.*, 2008, **22**, 1484–1490.

44 C. R. Kaze, S. Tome, G. L. Lecomte-Nana, A. Adesina, H. Essaedi, S. K. Das, T. Alomayri, E. Kamseu and U. C. Melo, *Materialia*, 2021, **15**, 101032.
45 C.-S. Poon, L. Lam, S. Kou, Y.-L. Wong and R. Wong, *Cem. Concr. Res.*, 2001, **31**, 1301–1306.
46 D. L. Kong, J. G. Sanjayan and K. Sagoe-Crentsil, *Cem. Concr. Res.*, 2007, **37**, 1583–1589.
47 C. Shi and J. Qian, *Resour., Conserv. Recycl.*, 2000, **29**, 195–207.
48 H.-W. Song and V. Saraswathy, *J. Hazard. Mater.*, 2006, **138**, 226–233.
49 J. C. Petermann, A. Saeed and M. I. Hammons, *Alkali-Activated Geopolymers: A Literature Review*, DTIC Document, 2010.
50 S. A. Bernal, J. L. Provis, B. Walkley, R. San Nicolas, J. D. Gehman, D. G. Brice, A. R. Kilcullen, P. Duxson and J. S. van Deventer, *Cem. Concr. Res.*, 2013, **53**, 127–144.
51 I. Ismail, S. A. Bernal, J. L. Provis, R. San Nicolas, S. Hamdan and J. S. van Deventer, *Cem. Concr. Compos.*, 2014, **45**, 125–135.
52 S. Kumar, R. Kumar and S. Mehrotra, *J. Mater. Sci.*, 2010, **45**, 607–615.
53 T. Cheng and J. Chiu, *Miner. Eng.*, 2003, **16**, 205–210.
54 P. Dinakar, K. P. Sethy and U. C. Sahoo, *Mater. Des.*, 2013, **43**, 161–169.
55 J. He, Y. Jie, J. Zhang, Y. Yu and G. Zhang, *Cem. Concr. Compos.*, 2013, **37**, 108–118.
56 D. Chaudhary and M. Jollands, *J. Appl. Polym. Sci.*, 2004, **93**, 1–8.
57 A. Muthadhi, R. Anitha and S. Kothandaraman, *J. Inst. Eng. (India), Civ. Eng. Div.*, 2007, **88**, 50–56.
58 S. Asavapisit and N. Ruengrit, *Cem. Concr. Compos.*, 2005, **27**, 782–787.
59 E. Basha, R. Hashim, H. Mahmud and A. Muntohar, *Constr. Build. Mater.*, 2005, **19**, 448–453.
60 L. Zhang, S. Ahmari and J. Zhang, *Constr. Build. Mater.*, 2011, **25**, 3773–3781.
61 J. Geng, M. Zhou, T. Zhang, W. Wang, T. Wang, X. Zhou, X. Wang and H. Hou, *Mater. Struct.*, 2017, **50**, 109.
62 D. González-García, L. Téllez-Jurado, F. Jiménez-Álvarez and H. Balmori-Ramírez, *Ceram. Int.*, 2017, **43**, 2606–2613.
63 H. Yildizay and R. Goren, *J. Aust. Ceram. Soc.*, 2017, 1–6.
64 Y. Djobo, A. Elimbi, J. D. Manga and I. D. L. Ndjock, *Constr. Build. Mater.*, 2016, **113**, 673–681.
65 P. Duan, C. Yan, W. Zhou and D. Ren, *Ceram. Int.*, 2016, **42**, 13507–13518.
66 B. Kord, *BioResources*, 2011, **6**, 1351–1358.
67 L. Vlaev, S. Turmanova and A. Dimitrova, *J. Polym. Res.*, 2009, **16**, 151–164.
68 S. Songpiriyakij, T. Kubprasit, C. Jaturapitakkul and P. Chindaprasirt, *Constr. Build. Mater.*, 2010, **24**, 236–240.
69 W. Sun, Y.-S. Zhang, W. Lin and Z.-Y. Liu, *Cem. Concr. Res.*, 2004, **34**, 935–940.
70 Y. Zhang, W. Sun and Z. Li, *Adv. Cem. Res.*, 2005, **17**, 23–28.
71 J. L. Provis and J. S. van Deventer, *Chem. Eng. Sci.*, 2007, **62**, 2309–2317.
72 Z. Zhang, H. Wang, J. L. Provis, F. Bullen, A. Reid and Y. Zhu, *Thermochim. Acta*, 2012, **539**, 23–33.
73 X. Yao, Z. Zhang, H. Zhu and Y. Chen, *Thermochim. Acta*, 2009, **493**, 49–54.
74 Z. Zhang, J. L. Provis, H. Wang, F. Bullen and A. Reid, *Thermochim. Acta*, 2013, **565**, 163–171.
75 C. E. White, K. Page, N. J. Henson and J. L. Provis, *Appl. Clay Sci.*, 2013, **73**, 17–25.
76 C. E. White, J. L. Provis, B. Bloomer, N. J. Henson and K. Page, *Phys. Chem. Chem. Phys.*, 2013, **15**, 8573–8582.
77 J. L. Provis, P. A. Walls and J. S. J. van Deventer, *Chem. Eng. Sci.*, 2008, **63**, 4480–4489.
78 C. A. Rees, J. L. Provis, G. C. Lukey and J. S. van Deventer, *Langmuir*, 2007, **23**, 8170–8179.
79 M. Zhang, M. Zhao, G. Zhang, T. El-Korchi and M. Tao, *Cem. Concr. Compos.*, 2017, **78**, 21–32.
80 Q. Wan, F. Rao, S. Song, R. E. García, R. M. Estrella, C. L. Patino and Y. Zhang, *Cem. Concr. Compos.*, 2017, **79**, 45–52.
81 G. Liang, W. Yao and A. She, *Cem. Concr. Compos.*, 2023, **137**, 104932.
82 M. Xia, H. Shi and X. Guo, *Mater. Lett.*, 2014, **136**, 222–224.
83 Z. Hu, M. Wyrzykowski and P. Lura, *Cem. Concr. Res.*, 2020, **129**, 105971.
84 C. Chen, W. Gong, W. Lutze and I. L. Pegg, *J. Mater. Sci.*, 2011, **46**, 3073–3083.
85 S. Chithiraputhiran and N. Neithalath, *Constr. Build. Mater.*, 2013, **45**, 233–242.
86 A. A. Siyal, K. A. Azizli, Z. Man, L. Ismail and M. I. Khan, *Ceram. Int.*, 2016, **42**, 15575–15584.
87 V. Glukhovsky, G. Rostovskaja and G. Rumyna, High strength slag-alkaline cements, in *Proceedings of the 7th International Congress on the Chemistry of Cement*, Paris, 1980.
88 J. Davidovits and J. Orlinski, *Geopolymer'88: First European Conference on Soft Mineralurgy*, 1st, 2nd, 3rd June 1988, The Institute, Compiègne, France, 1988.
89 J. Van Jaarsveld, J. Van Deventer and L. Lorenzen, *Metall. Mater. Trans. B*, 1998, **29**, 283–291.
90 A. Palomo, M. Grutzeck and M. Blanco, *Cem. Concr. Res.*, 1999, **29**, 1323–1329.
91 A. Hajimohammadi and J. S. van Deventer, *Int. J. Miner. Process.*, 2016, **153**, 80–86.
92 J. Davidovits, Geopolymer chemistry and properties, in *Geopolymer*, 1988, vol. 88, no. 1, pp. 25–48.
93 H. Xu and J. Van Deventer, *Int. J. Miner. Process.*, 2000, **59**, 247–266.
94 I. Ivanova, R. Aiello, J. Nagy, F. Crea, E. Derouane, N. Dumont, A. Nastro, B. Subotic and F. Testa, *Microporous Mater.*, 1994, **3**, 245–257.
95 G. Fernández and M. Luz, *Activación alcalina de metacaolín: desarrollo de nuevos materiales cementantes*, 1998.
96 S. Alonso and A. Palomo, *Cem. Concr. Res.*, 2001, **31**, 25–30.
97 D. Krizan and B. Zivanovic, *Cem. Concr. Res.*, 2002, **32**, 1181–1188.
98 J. Van Jaarsveld, J. Van Deventer and G. Lukey, *Chem. Eng. J.*, 2002, **89**, 63–73.

99 H. Xu and J. S. J. van Deventer, *Colloids Surf., A*, 2003, **216**, 27–44.
100 M. Criado, A. Palomo and A. Fernández-Jiménez, *Fuel*, 2005, **84**, 2048–2054.
101 J. Provis and J. Van Deventer, *Chem. Eng. Sci.*, 2007, **62**, 2318–2329.
102 J. Faimon, *Geochim. Cosmochim. Acta*, 1996, **60**, 2901–2907.
103 J. Provis, P. Duxson, J. Van Deventer and G. Lukey, *Chem. Eng. Res. Des.*, 2005, **83**, 853–860.
104 C. A. Rees, J. L. Provis, G. C. Lukey and J. S. van Deventer, *Colloids Surf., A*, 2008, **318**, 97–105.
105 K. Kupwade-Patil, S. O. Diallo, D. Z. Hossain, M. R. Islam and E. N. Allouche, *Constr. Build. Mater.*, 2016, **120**, 181–188.
106 S. Louati, S. Baklouti and B. Samet, *Appl. Clay Sci.*, 2016, **132**, 571–578.
107 S. Yan, P. He, D. Jia, X. Duan, Z. Yang, S. Wang and Y. Zhou, *RSC Adv.*, 2017, **7**, 13498–13508.
108 R. Aiello, F. Crea, A. Nastro, B. Subotić and F. Testa, *Zeolites*, 1991, **11**, 767–775.
109 X. Zhu, D. Yan, H. Fang, S. Chen and H. Ye, *Constr. Build. Mater.*, 2021, **266**, 121114.
110 P. Duxson, J. L. Provis, G. C. Lukey, F. Separovic and J. S. J. van Deventer, *Langmuir*, 2005, **21**, 3028–3036.
111 M. Zribi and S. Baklouti, *J. Non-Cryst. Solids*, 2021, **562**, 120777.
112 S. K. Nath and S. Kumar, *Adv. Powder Technol.*, 2019, **30**, 1079–1088.
113 H. Xu and J. S. van Deventer, *Colloids Surf., A*, 2003, **216**, 27–44.
114 P. De Silva and K. Sagoe-Crenstil, *J. Aust. Ceram. Soc.*, 2008, **44**, 39–46.
115 L. Zheng, W. Wang and Y. Shi, *Chemosphere*, 2010, **79**, 665–671.
116 P. Duxson, J. L. Provis, G. C. Lukey, F. Separovic and J. S. van Deventer, *Langmuir*, 2005, **21**, 3028–3036.
117 J. L. Provis, P. Duxson, G. C. Lukey and J. S. van Deventer, *Chem. Mater.*, 2005, **17**, 2976–2986.
118 F. Puertas, S. Martınez-Ramırez, S. Alonso and T. Vazquez, *Cem. Concr. Res.*, 2000, **30**, 1625–1632.
119 J. Van Jaarsveld, J. Van Deventer and G. Lukey, *Mater. Lett.*, 2003, **57**, 1272–1280.
120 D. Feng, H. Tan and J. Van Deventer, *J. Mater. Sci.*, 2004, **39**, 571–580.
121 H. A. Gasteiger, W. J. Frederick and R. C. Streisel, *Ind. Eng. Chem. Res.*, 1992, **31**, 1183–1190.
122 S. Alonso and A. Palomo, *Mater. Lett.*, 2001, **47**, 55–62.
123 C. Yip and J. Van Deventer, *J. Mater. Sci.*, 2003, **38**, 3851–3860.
124 C. K. Yip, G. Lukey and J. Van Deventer, *Cem. Concr. Res.*, 2005, **35**, 1688–1697.
125 D. Hardjito, S. E. Wallah, D. M. Sumajouw and B. V. Rangan, *ACI Mater. J.*, 2004, 101.
126 H. Xu and J. S. Van Deventer, *Miner. Eng.*, 2002, **15**, 1131–1139.
127 D. Sumajouw, D. Hardjito, S. Wallah and B. Rangan, Geopolymer concrete for a sustainable future, in *Proceedings of the Second International Conference on Sustainable Processing of Minerals and Metals, Green Processing*, 2004, vol. 2004.
128 J. Phair and J. Van Deventer, *Miner. Eng.*, 2001, **14**, 289–304.
129 R. Cioffi, L. Maffucci and L. Santoro, *Resour., Conserv. Recycl.*, 2003, **40**, 27–38.
130 H. Rahier, W. Simons, B. Van Mele and M. Biesemans, *J. Mater. Sci.*, 1997, **32**, 2237–2247.
131 R. Firdous and D. Stephan, *Constr. Build. Mater.*, 2019, **219**, 31–43.
132 D. Panias, I. P. Giannopoulou and T. Perraki, *Colloids Surf., A*, 2007, **301**, 246–254.
133 F. Škvára, J. Doležal, P. Svoboda, L. Kopecký, S. Pawlasová, M. Lucuk, K. Dvořáček, M. Beksa, L. Myšková and R. Šulc, *Proceedings of 16th IBAUSIL*, 2007, vol. 1, pp. 1079–1097.
134 I. Sinha and R. K. Mandal, *J. Non-Cryst. Solids*, 2011, **357**, 919–925.
135 R. Mohamed, R. Abd Razak, M. M. A. B. Abdullah, R. K. Shuib, Subaer and J. Chaiprapa, *J. Non-Cryst. Solids*, 2021, **553**, 120519.
136 A. Palomo, *Cem. Concr. Res.*, 2003, **33**, 281–288.
137 A. Kirschner and H. Harmuth, *Ceram.-Silik.*, 2004, **48**, 117–120.
138 F. Puertas, S. Martınez-Ramırez, S. Alonso and T. Vázquez, *Cem. Concr. Res.*, 2000, **30**, 1625–1632.
139 J. Temuujin, A. Van Riessen and R. Williams, *J. Hazard. Mater.*, 2009, **167**, 82–88.
140 T. Bakharev, *Cem. Concr. Res.*, 2005, **35**, 1224–1232.
141 M. Atkins, F. Glasser and J. Jack, *Waste Manage.*, 1995, **15**, 127–135.
142 M. Izquierdo, X. Querol, C. Phillipart, D. Antenucci and M. Towler, *J. Hazard. Mater.*, 2010, **176**, 623–628.
143 M. Granizo and M. Blanco, *J. Therm. Anal. Calorim.*, 1998, **52**, 957–965.
144 N. Granizo, A. Palomo and A. Fernandez-Jiménez, *Ceram. Int.*, 2014, **40**, 8975–8985.
145 A. Fernández-Jiménez and A. Palomo, *Cem. Concr. Res.*, 2005, **35**, 1984–1992.
146 D. Ravikumar, S. Peethamparan and N. Neithalath, *Cem. Concr. Compos.*, 2010, **32**, 399–410.
147 P. Wijnen, T. Beelen, J. De Haan, L. Van De Ven and R. Van Santen, *Colloids Surf.*, 1990, **45**, 255–268.
148 L. S. D. Glasser and G. Harvey, *J. Chem. Soc. Chem. Commun.*, 1984, 1250–1252.
149 A. Fernández-Jiménez and A. Palomo, *Fuel*, 2003, **82**, 2259–2265.
150 A. Palomo, S. Alonso, A. Fernandez-Jiménez, I. Sobrados and J. Sanz, *J. Am. Ceram. Soc.*, 2004, **87**, 1141–1145.
151 Z. Pan and J. G. Sanjayan, *Cem. Concr. Compos.*, 2012, **34**, 261–264.